JOURNAL OF GUIDANCE, CONTROL, AND DYNAMICS
Vol. 34, No. 5, September–October 2011

Linear Time-Varying Passivity-Based Attitude Control Employing Magnetic and Mechanical Actuation

James Richard Forbes* and Christopher John Damaren†
University of Toronto, Toronto, Ontario M3H 5T6, Canada

DOI: 10.2514/1.51899

Spacecraft attitude control using both magnetic and mechanical actuation is considered. Attitude control is composed of quaternion-based proportional control and passivity-based rate (angular velocity) control. A passivity-based scheme is adopted in order to guarantee robust closed-loop stability. Motivated by the nearly periodic nature of the Earth's magnetic field, a linear time-varying input strictly passive system is used within the rate control. Conditions that ensure a linear time-varying system is input strictly passive are given and are used in conjunction with the linear quadratic regulator formulation to design and synthesize the rate control. The attitude control formulation ensures that as time goes to infinity the spacecraft attitude and angular velocity go to zero. Simulation results are included that highlight the robust nature of the closed loop subject to both orbit and spacecraft model uncertainty.

I. Introduction

SPACECRAFT are usually equipped with some sort of attitude control system. Attitude control systems are usually required to enable pointing, slewing, or trajectory tracking (if not all these), as well as disturbance rejection. Although spacecraft in geocentric orbits can exploit environmental disturbance torques such as aerodynamic, gravity gradient, or those associated with solar-radiation pressure for attitude control or actuator desaturation, critical pointing is usually delegated to mechanical actuators, such as reaction wheels. Another viable actuation scheme enabling attitude control is magnetic actuation, whereby onboard magnetic dipole moments (created via current carrying coils) interact with the geomagnetic field, thereby creating torques [1,2].

All attitude control schemes that rely solely on magnetic actuation suffer from the same fundamental problem: instantaneous underactuation. A general control torque cannot be realized instantaneously by magnetic actuation alone, owing to the fact that the magnetic torque vector is generated via the cross-product of the magnetic field vector and the dipole moment vector. Although the stability of spacecraft equipped with magnetic actuators can be guaranteed on average [3–5], improved performance in terms of pointing accuracy is desired.

As a spacecraft orbits the Earth, the geomagnetic field properties relative to the spacecraft change in an (almost) periodic fashion. This periodic change has led many authors to investigate linear time-varying (LTV) or linear periodic control schemes to be used in conjunction with magnetic actuation [6–12]. For instance, [6–10] consider periodic state feedback control, while [11,12] consider periodic output feedback control. Some authors explicitly consider disturbance rejection in the design of their periodic control law [6,9]. Often, Floquet analysis is used to assess stability of the closed-loop system [7,8,10]; however, results that do not require a posteriori stability analysis are available [11,12].

Other authors have explored the use of tandem actuation, i.e., the collaborative use of magnetic and mechanical actuation, in order to, among other objectives, improve performance. References [13,14] consider spacecraft attitude control using reaction wheels and magnetic toque rods, while [15] uses thrusters and magnetic torque rods. Although both [13,14] use reaction wheels and magnetic torque rods in tandem, the control scheme of [13] allows for overlap of control torques, which is undesirable. The control architecture presented in [14] ensures that torques from each actuator are orthogonal, disallowing the possibility of having control torques overlap and in effect cancelling each other over short periods of time.

Tandem magnetic and mechanical actuation has also been used after hardware failures have occurred, to restore complete three-axis control, thus saving the mission in question. For example, the primary and secondary pitch axis wheels of RADARSAT-1 failed on orbit, thus rendering the pitch axis uncontrollable [16]. Similarly, the Far Ultraviolet Spectroscopic Explorer spacecraft experienced two reaction wheel failures (out of four), rendering three-axis control impossible [17]. In both scenarios, three-axis control was restored via some form of tandem magnetic and mechanical actuation.

The passivity theorem is one of the most famous and influential stability results applicable to both linear and nonlinear systems [18]. It states that a passive system and an input strictly passive system connected in negative feedback are stable. The passive nature of spacecraft has been exploited for control design enabling, for example, adaptive attitude control [19]. Passivity-based controllers possess excellent robustness properties. They are immune to modeling errors in, for example, the spacecraft mass distribution. Various authors have investigated LTV passive systems [20,21], yet there have been no examples of LTV input strictly passive systems being used as controllers in spacecraft applications.

This paper is concerned with passivity-based spacecraft attitude control subject to gravity-gradient disturbances. A passivity-based design approach is taken in order to guarantee robust closed-loop stability. The attitude controller is composed of quaternion-based proportional control and angular velocity based rate control. The rate controller employs an LTV input strictly passive system. Using an LTV system for control is motivated by the (almost) periodic nature of the linearized spacecraft model, for which the periodicity is a result of the magnetic field imposing its periodic nature upon the system. Both magnetic and mechanical actuation will be used, where the desired control torque will be distributed based on the physical constraints of the magnetic actuators. It is shown that the properties of the attitude controller ensure that both the vector part of the quaternion and the angular velocity go to zero as time goes to infinity.

After reviewing spacecraft kinematics, dynamics, etc., passive and input strictly passive systems are defined. A theorem is presented that

Presented as Paper 2010-7900 at the AIAA Guidance, Navigation, and Control Conference, Toronto, Ontario, Canada, 2–5 August 2010; received 5 August 2010; revision received 25 April 2011; accepted for publication 3 May 2011.

*Ph.D. Candidate, Institute for Aerospace Studies, 4925 Dufferin Street; forbes@utias.utoronto.ca. Student Member AIAA.

†Professor, Institute for Aerospace Studies, 4925 Dufferin Street; damaren@utias.utoronto.ca. Associate Fellow AIAA.

ensures an LTV system is input strictly passive. Controller design is then discussed, first showing that a spacecraft compensated by quaternion-based proportional control possesses a passive input–output map. A particular rate control that fosters an intuitive distribution of the control between both actuator sets is shown to be input strictly passive. An LTV input strictly passive controller design and synthesis method is presented that is based on a linearized model of the system being controlled. It is then shown that the attitude controller can robustly stabilize both the attitude and angular velocity of the spacecraft. Finally, a numerical example and closing remarks are given. Throughout the paper, the writing of the temporal argument of functions is neglected unless additional clarification is needed.

II. Spacecraft Kinematics, Dynamics, Disturbances, and Actuation

The rotational dynamics of generic rigid-body spacecraft in low Earth orbit are governed by Euler's equation (see [22], p. 95):

$$\mathbf{I}\,\dot{\boldsymbol{\omega}} + \boldsymbol{\omega}^{\times}\mathbf{I}\boldsymbol{\omega} = \boldsymbol{\tau}_d + \boldsymbol{\tau}_w + \boldsymbol{\tau}_m \tag{1}$$

where $\mathbf{I}$ is the moment of inertia matrix, $\boldsymbol{\omega}$ is the angular velocity of the spacecraft expressed in the body-fixed frame, $\boldsymbol{\tau}_d$ is the disturbance torque, and

$$\mathbf{a}^{\times} = \begin{bmatrix} 0 & -a_3 & a_2 \\ a_3 & 0 & -a_1 \\ -a_2 & a_1 & 0 \end{bmatrix}$$

is a skew-symmetric matrix satisfying $\mathbf{a}^{\times\top} = -\mathbf{a}^{\times}$ where $\mathbf{a} = [\,a_1 \quad a_2 \quad a_3\,]^{\top}$. The control torque $\mathbf{u}$ will be distributed between reaction wheel torques $\boldsymbol{\tau}_w$ and magnetic torques $\boldsymbol{\tau}_m(t) = \mathbf{b}^{\times\top}(t)\mathbf{m}(t)$, where $\mathbf{b}$ is the Earth's magnetic field vector expressed in the body-fixed frame, and $\mathbf{m}$ is the magnetic dipole moment [23]. The vector $\mathbf{b}$ is not constant as a result of the spacecraft changing position and attitude while on orbit. The geomagnetic field vector expressed in the inertial frame is $\mathbf{b}_i$, and $\mathbf{b} = \mathbf{C}_{bi}\mathbf{b}_i$ where $\mathbf{C}_{bi}$ is the rotation matrix from the inertial frame to the body-fixed frame.

We elect to neglect disturbance torques that arise via aerodynamics (which dominate at low altitudes) and solar-radiation pressure (which dominate at geostationary altitudes); the gravity-gradient torque will be considered the primary disturbance torque (see [22], pp. 233–239):

$$\boldsymbol{\tau}_d = \frac{3\mu}{|\mathbf{r}|^5}\mathbf{r}^{\times}\mathbf{I}\mathbf{r} \tag{2}$$

where $\mu = 3.98593 \times 10^{14}\ \mathrm{m}^3/\mathrm{s}^2$ is the Earth's gravitational constant, $\mathbf{r}$ is the position of the spacecraft relative to the Earth expressed in the spacecraft body frame, and $|\mathbf{r}| = \sqrt{\mathbf{r}^{\top}\mathbf{r}}$ is the Euclidean norm.

The attitude of a spacecraft can be described by the four-parameter quaternion set $\boldsymbol{\epsilon} = [\,\epsilon_1 \quad \epsilon_2 \quad \epsilon_3\,]^{\top}$ and η, which together satisfy $\boldsymbol{\epsilon}^{\top}\boldsymbol{\epsilon} + \eta^2 = 1$ (see [22], pp. 17, 26). The quaternion rates and the angular velocity are related by

$$\begin{bmatrix} \dot{\boldsymbol{\epsilon}} \\ \dot{\eta} \end{bmatrix} = \frac{1}{2}\begin{bmatrix} \eta\mathbf{1} + \boldsymbol{\epsilon}^{\times} \\ -\boldsymbol{\epsilon}^{\top} \end{bmatrix}\boldsymbol{\omega} \quad \text{or} \quad \boldsymbol{\omega} = 2[\,\eta\mathbf{1} - \boldsymbol{\epsilon}^{\times} \quad -\boldsymbol{\epsilon}\,]\begin{bmatrix} \dot{\boldsymbol{\epsilon}} \\ \dot{\eta} \end{bmatrix} \tag{3}$$

III. Linear Time-Varying Input Strictly Passive Systems

A function $\mathbf{u} \in L_2$ if $\|\mathbf{u}\|_2 = \sqrt{\int_0^{\infty}\mathbf{u}^{\top}(t)\mathbf{u}(t)\,\mathrm{d}t} < \infty$ and $\mathbf{u} \in L_{2e}$ if $\|\mathbf{u}\|_{2T} = \sqrt{\int_0^{T}\mathbf{u}^{\top}(t)\mathbf{u}(t)\,\mathrm{d}t} < \infty, \forall\ T \in \mathbb{R}^+$. A function $\mathbf{u} \in L_{\infty}$ if $\|\mathbf{u}\|_{\infty} = \sup_{t\in\mathbb{R}^+}[\max_{i=1\ldots n}|u_i(t)|] < \infty$. A general square system with inputs $\mathbf{u} \in L_{2e}$ and outputs $\mathbf{y} \in L_{2e}$ mapped through the operator $\mathcal{G}$: $L_{2e} \to L_{2e}$ is passive if there exists a constant β such that [19]

$$\int_0^T \mathbf{y}^{\top}(t)\mathbf{u}(t)\,\mathrm{d}t \geq \beta, \quad \forall\ \mathbf{u} \in L_{2e}, \quad \forall\ T \in \mathbb{R}^+ \tag{4}$$

and is input strictly passive if there exists β and $0 < \delta < \infty$ such that

$$\int_0^T \mathbf{y}^{\top}(t)\mathbf{u}(t)\,\mathrm{d}t \geq \delta\int_0^T \mathbf{u}^{\top}(t)\mathbf{u}(t)\,\mathrm{d}t + \beta, \quad \forall\ u \in L_{2e}, \quad \forall\ T \in \mathbb{R}^+ \tag{5}$$

The scalar β is related to the initial conditions of the system and takes on values less than or equal to zero. Formally, the simple version of the passivity theorem states that the negative feedback interconnection of a passive system and an input strictly passive system is L_2-stable [19].

In this paper, we will be concerned with square LTV systems of the form

$$\dot{\mathbf{x}}(t) = \mathbf{A}(t)\mathbf{x}(t) + \mathbf{B}(t)\mathbf{u}(t) \tag{6a}$$

$$\mathbf{y}(t) = \mathbf{C}(t)\mathbf{x}(t) + \mathbf{D}(t)\mathbf{u}(t) \tag{6b}$$

where $\mathbf{x} \in \mathbb{R}^n$, $\mathbf{u}, \mathbf{y} \in \mathbb{R}^m$, and the time-varying matrices $\mathbf{A}(\cdot)$, $\mathbf{B}(\cdot)$, $\mathbf{C}(\cdot)$, and $\mathbf{D}(\cdot)$ are appropriately dimensioned real matrices that are continuous. The nominal input–output equations are specified by Eqs. (6a) and (6b); an alternate output is

$$\mathbf{z}(t) = \mathbf{L}(t)\mathbf{x}(t) + \mathbf{W}(t)\mathbf{u}(t)$$

where $\mathbf{z} \in \mathbb{R}^m$. We will assume complete controllability of $[\mathbf{A}(\cdot), \mathbf{B}(\cdot)]$ and complete observability of $[\mathbf{C}(\cdot), \mathbf{A}(\cdot)]$ and $[\mathbf{L}(\cdot), \mathbf{A}(\cdot)]$ [24,25].

We will now consider input strictly passive LTV systems.

Theorem 3.1: an LTV system described by Eq. (6) that is completely controllable and completely observable with $\mathbf{D}(t) = \tilde{\mathbf{D}}(t) + \delta\mathbf{1}$ where $0 < \delta < \infty$ is input strictly passive if there exist continuous, bounded matrices $\mathbf{P}(t) = \mathbf{P}^{\top}(t) > 0$, $\mathbf{L}(\cdot)$, and $\mathbf{W}(\cdot)$ (where $[\mathbf{L}(\cdot), \mathbf{A}(\cdot)]$ is completely observable) such that

$$\dot{\mathbf{P}}(t) + \mathbf{P}(t)\mathbf{A}(t) + \mathbf{A}^{\top}(t)\mathbf{P}(t) = -\mathbf{L}^{\top}(t)\mathbf{L}(t) \tag{7a}$$

$$\mathbf{C}^{\top}(t) - \mathbf{P}(t)\mathbf{B}(t) = \mathbf{L}^{\top}(t)\mathbf{W}(t) \tag{7b}$$

$$\tilde{\mathbf{D}}(t) + \tilde{\mathbf{D}}^{\top}(t) = \mathbf{W}^{\top}(t)\mathbf{W}(t) \tag{7c}$$

Proof: to be concise, we will neglect writing the temporal argument of the input and output signals and time-varying matrices. Consider the following Lyapunov-like function and its temporal derivative:

$$V = \frac{1}{2}\mathbf{x}^{\top}\mathbf{P}\mathbf{x}$$

$$\dot{V} = \frac{1}{2}\mathbf{x}^{\top}\mathbf{P}\dot{\mathbf{x}} + \frac{1}{2}\dot{\mathbf{x}}^{\top}\mathbf{P}\mathbf{x} + \frac{1}{2}\mathbf{x}^{\top}\dot{\mathbf{P}}\mathbf{x} = \frac{1}{2}\mathbf{x}^{\top}(\dot{\mathbf{P}} + \mathbf{P}\mathbf{A} + \mathbf{A}^{\top}\mathbf{P})\mathbf{x} + \mathbf{x}^{\top}\mathbf{P}\mathbf{B}\mathbf{u}$$

Integrating $\dot{V}$ from 0 to T gives

$$\int_0^T \dot{V}\,\mathrm{d}t = V(T)\overbrace{-V(0)}^{\beta} \geq \beta$$

$$\int_0^T\left[\frac{1}{2}\mathbf{x}^{\top}(\dot{\mathbf{P}} + \mathbf{P}\mathbf{A} + \mathbf{A}^{\top}\mathbf{P})\mathbf{x} + \mathbf{x}^{\top}\mathbf{P}\mathbf{B}\mathbf{u}\right]\mathrm{d}t = \int_0^T\left[-\frac{1}{2}\mathbf{x}^{\top}\mathbf{L}^{\top}\mathbf{L}\mathbf{x} + \mathbf{x}^{\top}(\mathbf{C}^{\top} - \mathbf{L}^{\top}\mathbf{W})\mathbf{u}\right]\mathrm{d}t \geq \beta$$

$$\int_0^T \mathbf{x}^{\top}\mathbf{C}^{\top}\mathbf{u}\,\mathrm{d}t \geq \int_0^T\left(\frac{1}{2}\mathbf{x}^{\top}\mathbf{L}^{\top}\mathbf{L}\mathbf{x} + \mathbf{x}^{\top}\mathbf{L}^{\top}\mathbf{W}\mathbf{u}\right)\mathrm{d}t + \beta$$

where we have used Eqs. (7a) and (7b). Recall that $\mathbf{D}$ is square and can be broken up into symmetric and skew-symmetric parts: $\mathbf{D} = (1/2)(\mathbf{D} + \mathbf{D}^\top) + (1/2)(\mathbf{D} - \mathbf{D}^\top)$. Noting that

$$\mathbf{y}^\top\mathbf{u} = \mathbf{x}^\top\mathbf{C}^\top\mathbf{u} + \frac{1}{2}\mathbf{u}^\top(\mathbf{D}^\top + \mathbf{D})\mathbf{u} = \mathbf{x}^\top\mathbf{C}^\top\mathbf{u} + \frac{1}{2}\mathbf{u}^\top(\tilde{\mathbf{D}}^\top + \tilde{\mathbf{D}})\mathbf{u} + \delta\mathbf{u}^\top\mathbf{u} = \mathbf{x}^\top\mathbf{C}^\top\mathbf{u} + \frac{1}{2}\mathbf{u}^\top\mathbf{W}^\top\mathbf{W}\mathbf{u} + \delta\mathbf{u}^\top\mathbf{u}$$

where we have used Eq. (7c), we arrive at

$$\begin{aligned}\int_0^T \mathbf{y}^\top\mathbf{u}\ \mathrm{d}t &\geq \int_0^T \left(\frac{1}{2}\mathbf{x}^\top\mathbf{L}^\top\mathbf{L}\mathbf{x} + \mathbf{x}^\top\mathbf{L}^\top\mathbf{W}\mathbf{u} + \frac{1}{2}\mathbf{u}^\top\mathbf{W}^\top\mathbf{W}\mathbf{u} + \delta\mathbf{u}^\top\mathbf{u}\right)\mathrm{d}t + \beta \\ &= \frac{1}{2}\int_0^T (\mathbf{L}\mathbf{x} + \mathbf{W}\mathbf{u})^\top(\mathbf{L}\mathbf{x} + \mathbf{W}\mathbf{u})\ \mathrm{d}t \\ &\quad + \delta\int_0^T \mathbf{u}^\top\mathbf{u}\ \mathrm{d}t + \beta \geq \delta\int_0^T \mathbf{u}^\top\mathbf{u}\ \mathrm{d}t + \beta\end{aligned}$$

which completes the proof.

IV. Spacecraft Attitude Control Formulation

Neglecting the disturbance torque momentarily, consider a spacecraft endowed with three orthogonal reaction wheels and three orthogonal magnetic torque rods. The desired control torque $\mathbf{u}$ will be composed of proportional control $\mathbf{u}_p$ and rate control $\mathbf{u}_r$:

$$\mathbf{u} = \mathbf{u}_p + \mathbf{u}_r = \boldsymbol{\tau}_w + \boldsymbol{\tau}_m \tag{8}$$

How the desired control torque will be decomposed into wheel torques and magnetic torques will be discussed in Sec. IV.C.

A. Passivity Properties of a Spacecraft Compensated by Proportional Control

Proportional control of the form $\mathbf{u}_p = -k\boldsymbol{\epsilon}$ will be employed. In the following theorem, we will interpret the plant compensated by proportional control in terms of a passive input–output map between $\mathbf{u}_r$ and $\boldsymbol{\omega}$.

Theorem 4.1: a spacecraft described by Eqs. (1) and (3) (with $\boldsymbol{\tau}_d = \mathbf{0}$) compensated with proportional control of the form $\mathbf{u}_p = -k\boldsymbol{\epsilon}$ for $0 < k < \infty$ possesses a passive input–output map between $\mathbf{u}_r$ and $\boldsymbol{\omega}$.

Proof: consider the following Lyapunov-like function, its temporal derivative, and subsequent simplification [26]:

$$V = \frac{1}{2}\boldsymbol{\omega}^\top\mathbf{I}\boldsymbol{\omega} + k[\boldsymbol{\epsilon}^\top\boldsymbol{\epsilon} + (\eta - 1)^2]$$

$$\dot{V} = \boldsymbol{\omega}^\top(-\boldsymbol{\omega}^\times\mathbf{I}\boldsymbol{\omega} + \mathbf{u}_p + \mathbf{u}_r) + 2k[\boldsymbol{\epsilon}^\top\dot{\boldsymbol{\epsilon}} + (\eta - 1)\dot{\eta}] = -k\boldsymbol{\omega}^\top\boldsymbol{\epsilon} + \boldsymbol{\omega}^\top\mathbf{u}_r + k[\boldsymbol{\epsilon}^\top(\eta\mathbf{1} + \boldsymbol{\epsilon}^\times)\boldsymbol{\omega} - (\eta - 1)\boldsymbol{\epsilon}^\top\boldsymbol{\omega}] = \boldsymbol{\omega}^\top\mathbf{u}_r$$

where we have used Eq. (3) to simplify. Integrating the result between 0 and T delivers

$$\int_0^T \boldsymbol{\omega}^\top\mathbf{u}_r\ \mathrm{d}t = \int_0^T \dot{V}\ \mathrm{d}t = V(T) - V(0) \geq \overbrace{-V(0)}^{\beta}$$

which completes the proof.

Notice that the spacecraft compensated with proportional control is passive for any inertia matrix $\mathbf{I}$ and any positive k; the passive nature of the system does not hinge on particular numeric values.

B. Input Strictly Passive Rate Control

Given that a spacecraft compensated by proportional control is passive, stability of the spacecraft angular velocity can be guaranteed via the passivity theorem provided the rate controller (to be connected in a negative feedback loop) is input strictly passive. Note that only the angular velocity is guaranteed to be stable; stability of the attitude will be considered in Sec. IV.F.

The rate controller input is $\boldsymbol{\omega}$; the output is $\mathbf{v}_r = -\mathbf{u}_r$. Consider the following rate controller:

$$\mathbf{v}_r = \delta\hat{\mathbf{b}}\hat{\mathbf{b}}^\top\boldsymbol{\omega} + \hat{\mathbf{b}}^{\times\top}\boldsymbol{\mathcal{G}}(\hat{\mathbf{b}}^\times\boldsymbol{\omega}) \tag{9}$$

where $\hat{(\cdot)}$ denotes a unit vector (i.e., $\hat{\mathbf{b}} = |\mathbf{b}|^{-1}\mathbf{b}$), and $\boldsymbol{\mathcal{G}}$ is an input strictly passive operator satisfying Eq. (5). The δ in Eq. (9) is the same as the δ in Eq. (5) associated with $\boldsymbol{\mathcal{G}}$. In the following theorem, we will show that the map from $\boldsymbol{\omega}$ to $\mathbf{v}_r$ is input strictly passive.

Theorem 4.2: the map between $\boldsymbol{\omega}$ and $\mathbf{v}_r$ is input strictly passive; $\mathbf{v}_r$ is given in Eq. (9).

Proof: consider the following integral:

$$\begin{aligned}\int_0^T \boldsymbol{\omega}^\top\mathbf{v}_r\ \mathrm{d}t &= \int_0^T \boldsymbol{\omega}^\top[\delta\hat{\mathbf{b}}\hat{\mathbf{b}}^\top\boldsymbol{\omega} + \hat{\mathbf{b}}^{\times\top}\boldsymbol{\mathcal{G}}(\hat{\mathbf{b}}^\times\boldsymbol{\omega})]\ \mathrm{d}t \\ &\geq \delta\int_0^T \boldsymbol{\omega}^\top(\hat{\mathbf{b}}\hat{\mathbf{b}}^\top + \hat{\mathbf{b}}^{\times\top}\hat{\mathbf{b}}^\times)\boldsymbol{\omega}\ \mathrm{d}t + \beta \\ &= \delta\int_0^T \boldsymbol{\omega}^\top\boldsymbol{\omega}\ \mathrm{d}t + \beta\end{aligned}$$

where we have used the identity $\hat{\mathbf{b}}^{\times\top}\hat{\mathbf{b}}^\times = \mathbf{1} - \hat{\mathbf{b}}\hat{\mathbf{b}}^\top$ (see [22] pp. 58, 85).

C. Distribution of Control Between Wheel Torques and Magnetic Torques

The control torques applied to the spacecraft will be distributed as follows:

$$\mathbf{u} = \boldsymbol{\tau}_w + \boldsymbol{\tau}_m = \underbrace{\hat{\mathbf{b}}\hat{\mathbf{b}}^\top(-k\boldsymbol{\epsilon} - \delta\boldsymbol{\omega})}_{\boldsymbol{\tau}_w} + \underbrace{\hat{\mathbf{b}}^{\times\top}[-k\hat{\mathbf{b}}^\times\boldsymbol{\epsilon} - \boldsymbol{\mathcal{G}}(\hat{\mathbf{b}}^\times\boldsymbol{\omega})]}_{\boldsymbol{\tau}_m} \tag{10}$$

It is straightforward to have the reaction wheels apply the torque commanded to them, but the magnetic torques must be applied in the following way:

$$\boldsymbol{\tau}_m = \mathbf{b}^{\times\top}\mathbf{m}, \qquad \mathbf{m} = -|\mathbf{b}|^{-1}[k\hat{\mathbf{b}}^\times\boldsymbol{\epsilon} + \boldsymbol{\mathcal{G}}(\hat{\mathbf{b}}^\times\boldsymbol{\omega})]$$

The distribution presented in Eq. (10) can be interpreted in the following way using the results of [14]. Recall that the torque created by magnetic actuation is restricted to lie in a plane orthogonal to the instantaneous magnetic field vector. The preceding distribution distributes control torques such that any torque that lies in Ker $\{\mathbf{b}^\times\}$, i.e., parallel to $\mathbf{b}$, is applied by the reaction wheels. Torques that lie in Im $\{\mathbf{b}^\times\}$, i.e., perpendicular to $\mathbf{b}$, are applied by the magnetic torque rods.

Control torques are distributed in this tandem manner in order to reduce reaction wheel load. The overall load experienced by the reaction wheels is less (because the wheels are applying lower torques to the spacecraft), leading to longer wheel life or the use of smaller wheels. Depending on the spacecraft mission, ensuring longer wheel life may be more important (i.e., improving mission robustness and reliability). Alternatively, having smaller wheels may be desirable, especially in the context of micro- and nanosatellites. Smaller wheels may realize a reduced spacecraft mass, or the opportunity to increase the spacecraft payload.

D. Controller Design and Synthesis

Given the previously developed control formulation and decomposition, we are poised to design the input strictly passive operator $\boldsymbol{\mathcal{G}}$. Given that $\boldsymbol{\mathcal{G}}$ must be input strictly passive and the system to be controlled possesses periodic properties, $\boldsymbol{\mathcal{G}}$ will be realized by an input strictly passive LTV system and must satisfy theorem 3.1. We will design our controller $\boldsymbol{\mathcal{G}}$ based on a linearized model of the spacecraft to be controlled.

We will start by linearizing the spacecraft kinematics. We choose zero angular displacement and zero angular rate of the body-fixed

frame relative to the inertial frame as our linearization point. Assuming small angles and rates, we have $\boldsymbol{\theta} \doteq 2\boldsymbol{\epsilon}$, i.e., $\mathbf{C}_{bi} \doteq \mathbf{1} - \boldsymbol{\theta}^{\times}$, and $\dot{\boldsymbol{\theta}} \doteq \boldsymbol{\omega}$ (see [22], pp. 21–22, 27–29). Next, we will linearize the spacecraft dynamics. To do so, we will write the system to be controlled in the following way:

$$\mathbf{I}\,\dot{\boldsymbol{\omega}} + \boldsymbol{\omega}^{\times}\mathbf{I}\boldsymbol{\omega} = -k\boldsymbol{\epsilon} - \delta\hat{\mathbf{b}}\hat{\mathbf{b}}^{\top}\boldsymbol{\omega} + \hat{\mathbf{b}}^{\times\top}\mathbf{v} \tag{11a}$$

$$= -k\boldsymbol{\epsilon} - \delta\mathbf{C}_{bi}\hat{\mathbf{b}}_i\hat{\mathbf{b}}_i^{\top}\mathbf{C}_{bi}^{\top}\boldsymbol{\omega} + \mathbf{C}_{bi}\hat{\mathbf{b}}_i^{\times\top}\mathbf{C}_{bi}^{\top}\mathbf{v} \tag{11b}$$

where $\mathbf{v} = \mathcal{G}(\mathbf{y})$ and $\mathbf{y} = \hat{\mathbf{b}}^{\times}\boldsymbol{\omega} = \mathbf{C}_{bi}\hat{\mathbf{b}}_i^{\times}\mathbf{C}_{bi}^{\top}\boldsymbol{\omega}$ are the output and input of the input strictly passive LTV controller, respectively, and $\boldsymbol{\tau}_d = \mathbf{0}$. Note that we used the identity $(\mathbf{C}_{bi}\hat{\mathbf{b}}_i)^{\times} = \mathbf{C}_{bi}\hat{\mathbf{b}}_i^{\times}\mathbf{C}_{bi}^{\top}$ (see [22], pp. 529). Substitution of the linearized kinematics into Eq. (11) gives

$$\mathbf{I}\ddot{\boldsymbol{\theta}} + \dot{\boldsymbol{\theta}}^{\times}\mathbf{I}\dot{\boldsymbol{\theta}} = -\frac{k}{2}\boldsymbol{\theta} - \delta(\mathbf{1} - \boldsymbol{\theta}^{\times})\hat{\mathbf{b}}_i\hat{\mathbf{b}}_i^{\top}(\mathbf{1} - \boldsymbol{\theta}^{\times})^{\top}\dot{\boldsymbol{\theta}} + (\mathbf{1} - \boldsymbol{\theta}^{\times})\hat{\mathbf{b}}_i^{\times\top}(\mathbf{1} - \boldsymbol{\theta}^{\times})^{\top}\mathbf{v} \tag{12}$$

By neglecting terms that are of an order greater than one, Eq. (12) becomes

$$\mathbf{I}\,\ddot{\boldsymbol{\theta}} = -\frac{k}{2}\boldsymbol{\theta} - \delta\hat{\mathbf{b}}_i\hat{\mathbf{b}}_i^{\top}\dot{\boldsymbol{\theta}} + \hat{\mathbf{b}}_i^{\times\top}\mathbf{v}$$

which can be written in conjunction with $\mathbf{y} \doteq \hat{\mathbf{b}}_i^{\times}\dot{\boldsymbol{\theta}}$ in first-order state-space form:

$$\begin{bmatrix}\dot{\boldsymbol{\theta}}\\ \ddot{\boldsymbol{\theta}}\end{bmatrix} = \underbrace{\begin{bmatrix}\mathbf{0} & \mathbf{1}\\ -\frac{k}{2}\mathbf{I}^{-1} & -\delta\mathbf{I}^{-1}\hat{\mathbf{b}}_i\hat{\mathbf{b}}_i^{\top}\end{bmatrix}}_{\mathbf{A}(t)}\underbrace{\begin{bmatrix}\boldsymbol{\theta}\\ \dot{\boldsymbol{\theta}}\end{bmatrix}}_{\mathbf{x}(t)} + \underbrace{\begin{bmatrix}\mathbf{0}\\ \mathbf{I}^{-1}\hat{\mathbf{b}}_i^{\times\top}\end{bmatrix}}_{\mathbf{B}(t)}\mathbf{v}(t) \tag{13a}$$

$$\mathbf{y}(t) = \underbrace{\begin{bmatrix}\mathbf{0} & \hat{\mathbf{b}}_i^{\times}\end{bmatrix}}_{\mathbf{C}(t)}\begin{bmatrix}\boldsymbol{\theta}\\ \dot{\boldsymbol{\theta}}\end{bmatrix} \tag{13b}$$

Equation (13) is the linearized plant model. We have written the temporal arguments in Eq. (13) to emphasize the linear model is time-varying.

The input strictly passive controller $\mathcal{G}$ to be designed based on Eq. (13) can be expressed in terms of a minimal state-space realization:

$$\dot{\mathbf{x}}_c(t) = \mathbf{A}_c(t)\mathbf{x}_c(t) + \mathbf{B}_c(t)\mathbf{y}(t) \tag{14a}$$

$$\mathbf{v}(t) = \mathbf{C}_c(t)\mathbf{x}_c(t) + \mathbf{D}_c(t)\mathbf{y}(t) \tag{14b}$$

Rather then arbitrarily assigning the $\mathbf{A}_c(\cdot)$ and $\mathbf{C}_c(\cdot)$ matrices, we will design them via the well-known linear quadratic regulator (LQR) formulation. Given the performance index [27,28]

$$\mathcal{J} = \mathbf{x}^{\top}(T)\mathbf{S}\mathbf{x}(T) + \int_0^T [\mathbf{x}^{\top}(t)\mathbf{M}\mathbf{x}(t) + \mathbf{v}^{\top}(t)\mathbf{N}\mathbf{v}(t)]\,\mathrm{d}t$$

where $\mathbf{S} = \mathbf{S}^{\top} \geq 0, \mathbf{M} = \mathbf{M}^{\top} \geq 0$, and $\mathbf{N} = \mathbf{N}^{\top} > 0$, one can derive an optimal-state feedback $\mathbf{C}_c(t) = \mathbf{N}^{-1}\mathbf{B}^{\top}(t)\mathbf{X}(t)$. The matrix $\mathbf{X}(\cdot) = \mathbf{X}^{\top}(\cdot) \geq 0$ can be found by solving the following time-varying matrix Riccati equation:

$$-\dot{\mathbf{X}}(t) = \mathbf{M} + \mathbf{A}^{\top}(t)\mathbf{X}(t) + \mathbf{X}(t)\mathbf{A}(t) - \mathbf{X}(t)\mathbf{B}(t)\mathbf{N}^{-1}\mathbf{B}^{\top}(t)\mathbf{X}(t),$$
$$\mathbf{X}(T) = \mathbf{S} \tag{15}$$

The matrix Riccati equation must be solved backward in time from $t = T$ to $t = 0$ given the boundary condition $\mathbf{X}(T) = \mathbf{S}$. Following the LQR formulation, we will let $\mathbf{A}_c(t) = \mathbf{A}(t) - \mathbf{B}(t)\mathbf{C}_c(t)$. Given that we have specified $\mathbf{A}_c(\cdot)$ and $\mathbf{C}_c(\cdot)$, we must now design $\mathbf{B}_c(\cdot)$ and $\mathbf{D}_c(\cdot)$ such that the controller is input strictly passive according to theorem 3.1. By specifying $\mathbf{L}(\cdot)$ appropriately, i.e., so that $[\mathbf{L}(\cdot), \mathbf{A}_c(\cdot)]$ is observable, and $\mathbf{D}_c(\cdot)$ to be positive definite [or alternatively $\tilde{\mathbf{D}}(\cdot)$, which in turn dictates $\mathbf{W}(\cdot)$], the matrix $\mathbf{B}_c(\cdot)$ can be solved for via Eq. (7b):

$$\mathbf{B}_c(t) = \mathbf{P}^{-1}(t)[\mathbf{C}_c^{\top}(t) - \mathbf{L}^{\top}(t)\mathbf{W}(t)]$$

where $\mathbf{P}(\cdot)$ is found by solving Eq. (7a):

$$\dot{\mathbf{P}}(t) + \mathbf{P}(t)\mathbf{A}_c(t) + \mathbf{A}_c^{\top}(t)\mathbf{P}(t) = -\mathbf{L}^{\top}(t)\mathbf{L}(t) \tag{16}$$

backwards in time from $t = T$ to $t = 0$ given the boundary condition $\mathbf{P}(T) > 0$. To compute $\mathbf{B}_c(\cdot)$, the matrix $\mathbf{P}(\cdot)$ must be inverted, which is why $[\mathbf{A}_c(\cdot), \mathbf{B}_c(\cdot)]$ must be completely controllable and the pairs $[\mathbf{C}_c(\cdot), \mathbf{A}_c(\cdot)]$ and $[\mathbf{L}(\cdot), \mathbf{A}_c(\cdot)]$ must be completely observable [20,21].

The resultant $\mathbf{A}_c(\cdot)$, $\mathbf{B}_c(\cdot)$, $\mathbf{C}_c(\cdot)$, and $\mathbf{D}_c(\cdot)$ compose an input strictly passive controller of the form presented in Eq. (14). The synthesis procedure will always yield an input strictly passive operator $\mathcal{G}$, even if the assumed spacecraft inertia matrix $\mathbf{I}$ and orbit (and hence $\mathbf{b}_i$ values) are incorrect.

E. Practical Considerations and Additional Comments

Some remarks with respect to implementation of the proposed control architecture are in order. To start, recall the linearized system in Eq. (13), which is used as the basis for controller design. Indeed, the linearized system is time-varying, but owing to the presence of terms involving the Earth's magnetic field vector $\mathbf{b}_i$ the linearized system is in fact approximately periodic. As such, it is expected that upon backward integration of Eqs. (15) and (16) the matrices $\mathbf{X}(\cdot)$ and $\mathbf{P}(\cdot)$ will have a steady state that is approximately periodic as well.

It is unreasonable to store the steady-state solutions of $\mathbf{X}(\cdot)$ and $\mathbf{P}(\cdot)$ (from $t = 0$ to $t = T$) onboard the spacecraft. Given that $\mathbf{X}(\cdot)$ and $\mathbf{P}(\cdot)$ have almost periodic steady-state solutions, in practice the upper (or lower) triangular parts of $\mathbf{X}(\cdot)$ and $\mathbf{P}(\cdot)$ would be approximated by a Fourier series. (Recall, $\mathbf{X}(\cdot)$ and $\mathbf{P}(\cdot)$ are symmetric, hence approximating every element of the matrices is unnecessary.) The Fourier coefficients associated with each Fourier series used to approximate the appropriate elements of $\mathbf{X}(\cdot)$ and $\mathbf{P}(\cdot)$ would then be stored onboard. Other approximations may be used; [6] suggests using a spline approximation.

F. Convergence of Attitude and Angular Velocity to Zero

We will now show that as time goes to infinity, $\boldsymbol{\epsilon}$ and $\boldsymbol{\omega}$ go to zero. To do so, we will first show that the input strictly passive operator $\mathcal{G}$ designed by the method outlined in Sec. IV.D satisfies two critical properties related to boundedness and convergence. We will then show that $\boldsymbol{\epsilon}, \eta$, and $\boldsymbol{\omega} \in L_{\infty}$, which will lead to $\boldsymbol{\omega}(t) \to \mathbf{0}$ as $t \to \infty$. Finally, using an invariance result associated with asymptotically autonomous systems [29], we will show that $\boldsymbol{\epsilon}(t) \to \mathbf{0}$ as $t \to \infty$.

We will begin by showing that the map $\mathbf{v} = \mathcal{G}(\mathbf{y})$ has the following properties: 1) $\mathbf{y} \in L_{\infty} \Rightarrow \mathbf{v} \in L_{\infty}$ and 2) $\mathbf{y} \in L_2$ and $\mathbf{y}(t) \to \mathbf{0}$ as $t \to \infty \Rightarrow \mathbf{v}(t) \to \mathbf{0}$ as $t \to \infty$.

To show that $\mathbf{v} = \mathcal{G}(\mathbf{y})$ satisfies property 1, first consider the solution of Eq. (14):

$$\mathbf{x}_c(t) = \boldsymbol{\Phi}(t, 0)\mathbf{x}_c(0) + \int_0^t \boldsymbol{\Phi}(t, \tau)\mathbf{B}_c(\tau)\mathbf{y}(\tau)\,\mathrm{d}\tau$$
$$\mathbf{v}(t) = \mathbf{C}_c(t)\mathbf{x}_c(t) + \mathbf{D}_c(t)\mathbf{y}(t)$$

where $\boldsymbol{\Phi}(\cdot, \cdot)$ is the state-transition matrix associated with the homogeneous system $\dot{\mathbf{x}}_c(t) = \mathbf{A}_c(t)\mathbf{x}_c(t)$ with solution $\mathbf{x}_c(t) = \boldsymbol{\Phi}(t, 0)\mathbf{x}_c(0)$. We have designed $\mathbf{A}_c(\cdot)$ using a LQR formulation; a Lyapunov-type analysis can be used to show that solutions of $\dot{\mathbf{x}}_c(t) = \mathbf{A}_c(t)\mathbf{x}_c(t)$ satisfy

$$|\mathbf{x}_c(t_2)| \leq Ke^{-a(t_2 - t_1)}|\mathbf{x}_c(t_1)|$$

where $0 < K < \infty$ and $0 < a < \infty$, which is to say the system is exponentially stable [30]. Using this fact, we can show that the state-transition matrix is bounded:

$$\|\boldsymbol{\Phi}(t_2, t_1)\| = \max_{|\mathbf{x}_c(t_1)|=1} |\boldsymbol{\Phi}(t_2, t_1)\mathbf{x}_c(t_1)|$$
$$= \max_{|\mathbf{x}_c(t_1)|=1} |\mathbf{x}_c(t_2)| \leq Ke^{-a(t_2-t_1)} \tag{17}$$

where $\|\mathbf{X}\| = \sqrt{\bar{\lambda}\{\mathbf{X}^\top\mathbf{X}\}}$ is the induced matrix norm and $\bar{\lambda}\{\cdot\}$ is the maximum eigenvalue. Next, recall that $\mathbf{y} \in L_\infty$, and each of the matrices $\mathbf{A}_c(\cdot)$, $\mathbf{B}_c(\cdot)$, $\mathbf{C}_c(\cdot)$, and $\mathbf{D}_c(\cdot)$ is bounded. As such, let $|\mathbf{y}(t)| \leq \bar{y}$, $\|\mathbf{A}_c(t)\| \leq \bar{A}_c$, $\|\mathbf{B}_c(t)\| \leq \bar{B}_c$, $\|\mathbf{C}_c(t)\| \leq \bar{C}_c$, and $\|\mathbf{D}_c(t)\| \leq \bar{D}_c \ \ \forall\ t \in \mathbb{R}^+$. Also, partition the nonhomogeneous solutions of $\mathbf{x}_c(\cdot)$ as follows:

$$\mathbf{x}_c(t) = \mathbf{x}_{c1}(t) + \mathbf{x}_{c2}(t), \qquad \mathbf{x}_{c1}(t) = \boldsymbol{\Phi}(t, 0)\mathbf{x}_c(0)$$
$$\mathbf{x}_{c2}(t) = \int_0^t \boldsymbol{\Phi}(t, \tau)\mathbf{B}_c(\tau)\mathbf{y}(\tau)\ \mathrm{d}\tau \tag{18}$$

To show that $\mathbf{y} \in L_\infty$ implies $\mathbf{v} \in L_\infty$, we will first show that $\mathbf{x}_{c1}(\cdot)$ and $\mathbf{x}_{c2}(\cdot)$ are in L_∞, which will lead to the desired result. As such, consider the Euclidean norm of $\mathbf{x}_{c1}(\cdot)$:

$$|\mathbf{x}_{c1}(t)| \leq |\boldsymbol{\Phi}(t, 0)\mathbf{x}_c(0)| \leq Ke^{-at}|\mathbf{x}_c(0)| \leq K|\mathbf{x}_c(0)|$$

where the inequality in Eq. (17) has been used. This shows that $\mathbf{x}_{c1}(\cdot)$ is bounded, and hence $\mathbf{x}_{c1} \in L_\infty$. To show $\mathbf{x}_{c2} \in L_\infty$ consider the following:

$$|\mathbf{x}_{c2}(t)| = |\int_0^t \boldsymbol{\Phi}(t, \tau)\mathbf{B}_c(\tau)\mathbf{y}(\tau)\ \mathrm{d}\tau| \leq \int_0^t |\boldsymbol{\Phi}(t, \tau)\mathbf{B}_c(\tau)\mathbf{y}(\tau)|\ \mathrm{d}\tau$$
$$\leq K\bar{B}_c\bar{y}\int_0^t e^{-a(t-\tau)}\ \mathrm{d}\tau \leq \frac{K\bar{B}_c\bar{y}}{a}$$

where we have used the inequality in Eq. (17) once again. This shows that $\mathbf{x}_{c2}(\cdot)$ is bounded as well, and hence $\mathbf{x}_{c2} \in L_\infty$. Given that $\mathbf{x}_{c1}$, $\mathbf{x}_{c2} \in L_\infty$, then $\mathbf{x}_c \in L_\infty$ as well. Using Eq. (14b), the fact that $\mathbf{y}$, $\mathbf{x}_c \in L_\infty$, and the boundedness of $\mathbf{C}_c(\cdot)$ and $\mathbf{D}_c(\cdot)$, yields $\mathbf{v} \in L_\infty$.

Next, we will show that $\mathbf{v} = \mathcal{G}(\mathbf{y})$ satisfies property 2. We will first show that $\mathbf{x}_c \in L_2$. Consider the decomposition of $\mathbf{x}_c(\cdot)$ in Eq. (18) once more. The square of the L_2 norm of $\mathbf{x}_{c1}(\cdot)$ is

$$\|\mathbf{x}_{c1}\|_2^2 = \int_0^\infty |\boldsymbol{\Phi}(t, 0)\mathbf{x}_c(0)|^2\ \mathrm{d}t \leq \int_0^\infty \|\boldsymbol{\Phi}(t, 0)\|^2|\mathbf{x}_c(0)|^2\ \mathrm{d}t$$
$$\leq K^2|\mathbf{x}_c(0)|^2\int_0^\infty e^{-2at}\ \mathrm{d}t = \frac{K^2|\mathbf{x}_c(0)|^2}{2a}$$

Thus, $\mathbf{x}_{c1} \in L_2$. Now, consider the Euclidean norm of $\mathbf{x}_{c2}(\cdot)$:

$$|\mathbf{x}_{c2}(t)| \leq \int_0^t |\boldsymbol{\Phi}(t, \tau)\mathbf{B}_c(\tau)\mathbf{y}(\tau)|\ \mathrm{d}\tau \leq K\bar{B}_c\int_0^t e^{-a(t-\tau)}|\mathbf{y}(\tau)|\ \mathrm{d}\tau$$
$$= K\bar{B}_c\int_0^t (e^{-a(t-\tau)}|\mathbf{y}(\tau)|^2)^{\frac{1}{2}}(e^{-a(t-\tau)})^{\frac{1}{2}}\ \mathrm{d}\tau$$

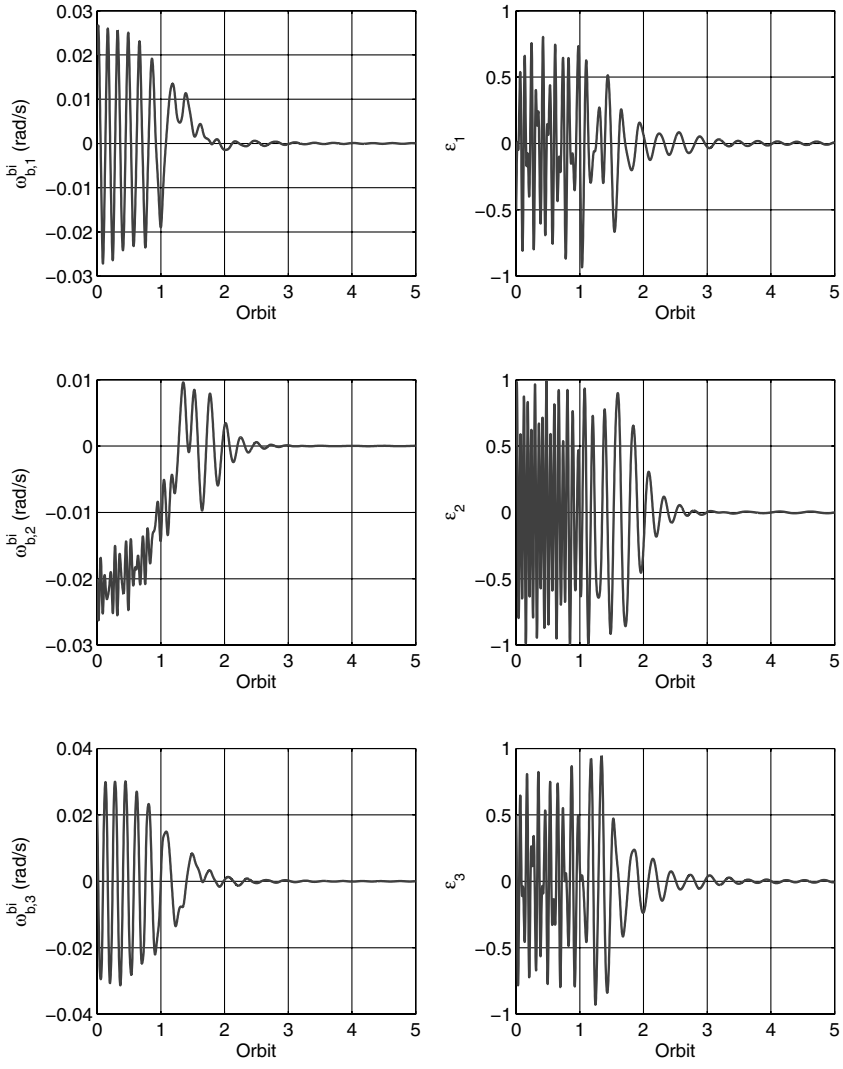

Fig. 1 Angular velocity and quaternions vs orbit.

By using Hölder's inequality, we then have

$$|\mathbf{x}_{c2}(t)| \le K\bar{B}_c\left[\int_0^t e^{-a(t-\tau)}|\mathbf{y}(\tau)|^2\,\mathrm{d}\tau\right]^{\frac{1}{2}}\left[\int_0^t e^{-a(t-\tau)}\,\mathrm{d}\tau\right]^{\frac{1}{2}}$$
$$\le \frac{K\bar{B}_c}{a}\left[\int_0^t e^{-a(t-\tau)}|\mathbf{y}(\tau)|^2\,\mathrm{d}\tau\right]^{\frac{1}{2}}$$

Squaring both sides and integrating between $t = 0$ and $t = T$ gives

$$\|\mathbf{x}_{c2}\|_{2T}^2 \le \frac{K^2\bar{B}_c^2}{a^2}\int_0^T\int_0^t e^{-a(t-\tau)}|\mathbf{y}(\tau)|^2\,\mathrm{d}\tau\,\mathrm{d}t$$
$$= \frac{K^2\bar{B}_c^2}{a^2}\int_0^T\int_\tau^T e^{-a(t-\tau)}|\mathbf{y}(\tau)|^2\,\mathrm{d}t\,\mathrm{d}\tau \tag{19}$$

where we have changed the bounds of integration on the right-hand side of the inequality. The integral $\int_\tau^T e^{-a(t-\tau)}\,\mathrm{d}t$ is bounded by $1/a$; the inequality in Eq. (19) becomes

$$\|\mathbf{x}_{c2}\|_{2T}^2 \le \frac{K^2\bar{B}_c^2}{a^3}\|\mathbf{y}\|_{2T}^2$$

Taking the square root of each side of the preceding inequality and letting $T \to \infty$ yields $\mathbf{x}_{c2} \in L_2$. Because $\mathbf{x}_{c1}$, $\mathbf{x}_{c2} \in L_2$, $\mathbf{x}_c \in L_2$. Now, from Eq. (14a), because both $\mathbf{A}_c(\cdot)$ and $\mathbf{B}_c(\cdot)$ are both bounded, we have $\dot{\mathbf{x}}_c \in L_2$ as well. Because $\mathbf{x}_c$, $\dot{\mathbf{x}}_c \in L_2$, $\mathbf{x}(t) \to \mathbf{0}$ as $t \to \infty$ [31]. Because $\mathbf{y}(t) \to \mathbf{0}$ and $\mathbf{x}_c(t) \to \mathbf{0}$ as $t \to \infty$, from Eq. (14b) we then have that $\mathbf{v}(t) \to \mathbf{0}$.

Having established that $\mathbf{v} = \mathcal{G}(\mathbf{y})$ satisfies both properties 1 and 2, let us now turn our attention to the closed-loop system. Combining the plant dynamics, kinematics, and control given in Eqs. (1), (3), and (8) [i.e., $\mathbf{u}_p = -k\boldsymbol{\epsilon}$ and $\mathbf{u}_r = -\mathbf{v}_r$; $\mathbf{v}_r$ is given in Eq. (9)], the undisturbed closed-loop system is described by

$$\dot{\boldsymbol{\epsilon}} = \frac{1}{2}(\eta\mathbf{1} + \boldsymbol{\epsilon}^\times)\boldsymbol{\omega} \tag{20a}$$

$$\dot{\eta} = -\frac{1}{2}\boldsymbol{\epsilon}^\top\boldsymbol{\omega} \tag{20b}$$

$$\mathbf{I}\,\dot{\boldsymbol{\omega}} = -k\boldsymbol{\epsilon} + \mathbf{h}(\boldsymbol{\omega}, t) \tag{20c}$$

where

$$\mathbf{h}(\boldsymbol{\omega}, t) = -\boldsymbol{\omega}^\times\mathbf{I}\boldsymbol{\omega} - \delta\hat{\mathbf{b}}\hat{\mathbf{b}}^\top\boldsymbol{\omega} - \hat{\mathbf{b}}^{\times\top}\mathcal{G}(\hat{\mathbf{b}}^\times\boldsymbol{\omega}) \tag{21}$$

We will now show that $\boldsymbol{\epsilon}$, η, and $\boldsymbol{\omega} \in L_\infty$. Consider once again the Lypaunov-like function used previously in the proof of theorem 4.1, its temporal derivative, and subsequent simplification:

$$V = \frac{1}{2}\boldsymbol{\omega}^\top\mathbf{I}\boldsymbol{\omega} + k[\boldsymbol{\epsilon}^\top\boldsymbol{\epsilon} + (\eta - 1)^2]$$
$$\dot{V} = -\boldsymbol{\omega}^\top[\delta\hat{\mathbf{b}}\hat{\mathbf{b}}^\top\boldsymbol{\omega} - \hat{\mathbf{b}}^{\times\top}\mathcal{G}(\hat{\mathbf{b}}^\times\boldsymbol{\omega})]$$

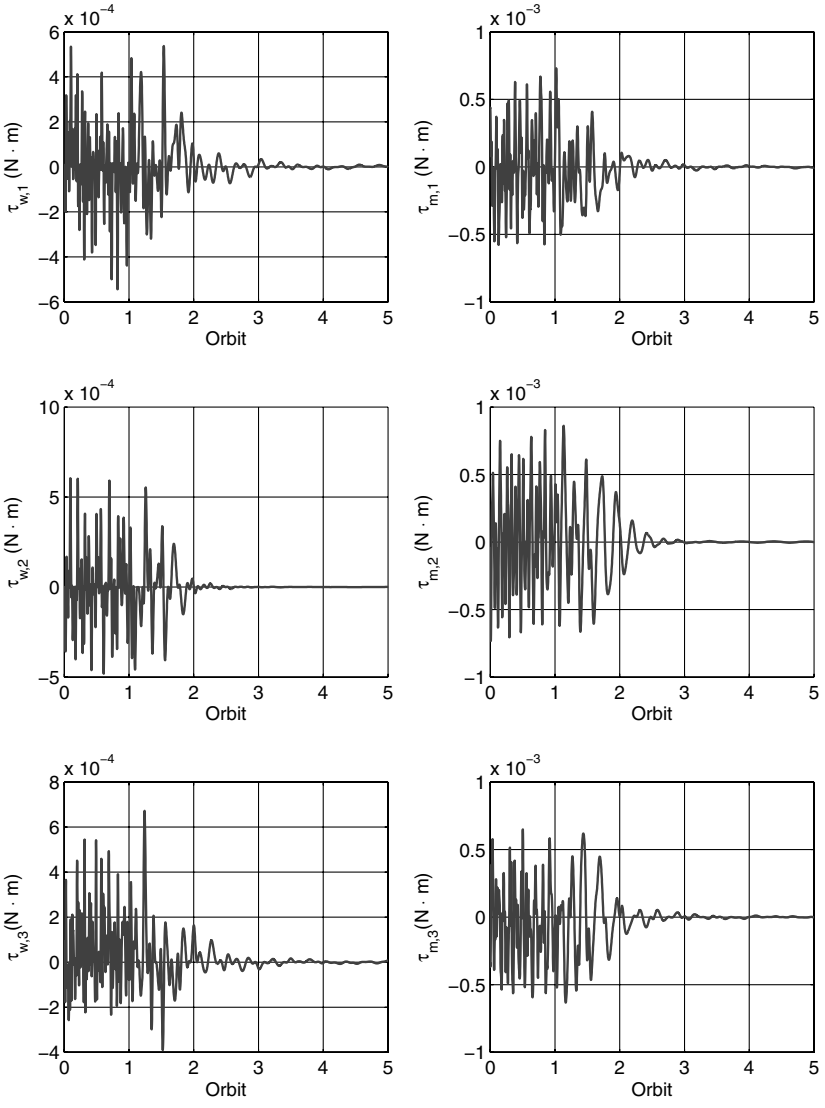

Fig. 2 Wheel torque and magnetic torque vs orbit.

Integrating $\dot{V}$ between 0 and t and using the fact that $\mathcal{G}$ is input strictly passive gives

$$V(t) - V(0) = -\int_0^t \boldsymbol{\omega}^\top [\delta \hat{\mathbf{b}}\hat{\mathbf{b}}^\top \boldsymbol{\omega} - \hat{\mathbf{b}}^{\times\top} \mathcal{G}(\hat{\mathbf{b}}^\times \boldsymbol{\omega})]\, \mathrm{d}\tau$$
$$\leq -\delta \int_0^t \boldsymbol{\omega}^\top \boldsymbol{\omega}\, \mathrm{d}\tau - \beta$$

Rearranging, we have

$$V(t) \leq V(0) - \delta \int_0^t \boldsymbol{\omega}^\top \boldsymbol{\omega}\, \mathrm{d}\tau - \beta \leq V(0) - \beta \tag{22}$$

where $-\beta \geq 0$. Clearly, V is bounded from above, and as a result $\boldsymbol{\epsilon}, \eta$, and $\boldsymbol{\omega}$ are bounded as well. Hence, $\boldsymbol{\epsilon}$, η, and $\boldsymbol{\omega} \in L_\infty$. Using the inequality in Eq. (22) we can also confirm that $\boldsymbol{\omega} \in L_2$:

$$\delta \int_0^T \boldsymbol{\omega}^\top \boldsymbol{\omega}\, \mathrm{d}t \leq V(0) - \beta$$

Letting T go to infinity confirms $\boldsymbol{\omega} \in L_2$, a result already ensured by the passivity theorem.

Having shown that $\boldsymbol{\epsilon}$, η, and $\boldsymbol{\omega} \in L_\infty$, we will now show that $\boldsymbol{\omega}(t) \to \mathbf{0}$ as $t \to \infty$. Because $\boldsymbol{\omega} \in L_\infty$, $\hat{\mathbf{b}}^\times \boldsymbol{\omega} \in L_\infty$. From property 1, we have that $\mathcal{G}(\hat{\mathbf{b}}^\times \boldsymbol{\omega}) \in L_\infty$. Because $\boldsymbol{\epsilon}$ and $\boldsymbol{\omega} \in L_\infty$, from Eqs. (20c) and (21) we have that $\dot{\boldsymbol{\omega}} \in L_\infty$ as well. Given that $\boldsymbol{\omega} \in L_2$ and $\dot{\boldsymbol{\omega}} \in L_\infty$, from Barbalat's lemma [32] we conclude that $\boldsymbol{\omega}(t) \to \mathbf{0}$ as $t \to \infty$.

Our last challenge is to show that $\boldsymbol{\epsilon}$ goes to zero as time goes to infinity. Owing to the fact that $\mathcal{G}$ satisfies property 2 and $\boldsymbol{\omega}(t) \to \mathbf{0}$ as $t \to \infty$, it follows that $\mathbf{h}(\boldsymbol{\omega}, t) \to \mathbf{0}$ as $t \to \infty$ also. As such, all trajectories of the closed-loop system given in Eq. (20) approach the set $\Omega = [(\boldsymbol{\epsilon}, \eta, \boldsymbol{\omega}) \in \mathbb{R}^3 \times \mathbb{R} \times \mathbb{R}^3 | \boldsymbol{\omega} = \mathbf{0}]$. Next, let $(\boldsymbol{\epsilon}, \eta, \boldsymbol{\omega})$ be a solution of Eq. (20) given some initial conditions. Using the results of [29], because $\mathbf{h}(\boldsymbol{\omega}, t) \to \mathbf{0}$, the nonautonomous system in Eq. (20) is asymptotically autonomous to

$$\dot{\bar{\boldsymbol{\epsilon}}} = \frac{1}{2}(\bar{\eta}\mathbf{1} + \bar{\boldsymbol{\epsilon}}^\times)\bar{\boldsymbol{\omega}} \tag{23a}$$

$$\dot{\bar{\eta}} = -\frac{1}{2}\bar{\boldsymbol{\epsilon}}^\top \bar{\boldsymbol{\omega}} \tag{23b}$$

$$\mathbf{I}\,\dot{\bar{\boldsymbol{\omega}}} = -k\bar{\boldsymbol{\epsilon}} \tag{23c}$$

which is an autonomous system. As such, the positive limit set of the system in Eq. (20) approaches the largest invariant set of the autonomous system in Eq. (23) contained in Ω. With $\boldsymbol{\omega} = \mathbf{0}$ and $\dot{\boldsymbol{\omega}} = \mathbf{0}$, from Eq. (23c) we have that $\boldsymbol{\epsilon} = \mathbf{0}$ as well. Therefore, we can conclude that $\boldsymbol{\epsilon}(t) \to \mathbf{0}$ as $t \to \infty$.

Given a system with quaternion-based proportional control and passivity-based rate control, we have shown that both $\boldsymbol{\epsilon}(t) \to \mathbf{0}$ and $\boldsymbol{\omega}(t) \to \mathbf{0}$ as $t \to \infty$. Of particular interest is the fact that convergence of $\boldsymbol{\epsilon}$ and $\boldsymbol{\omega}$ to zero does not hinge on the particular values of k and δ, nor particular $\mathbf{A}_c(\cdot)$, $\mathbf{B}_c(\cdot)$, $\mathbf{C}_c(\cdot)$, or $\mathbf{D}_c(\cdot)$ matrices. Provided that $0 < k < \infty, 0 < \delta < \infty$, and the synthesis procedure of

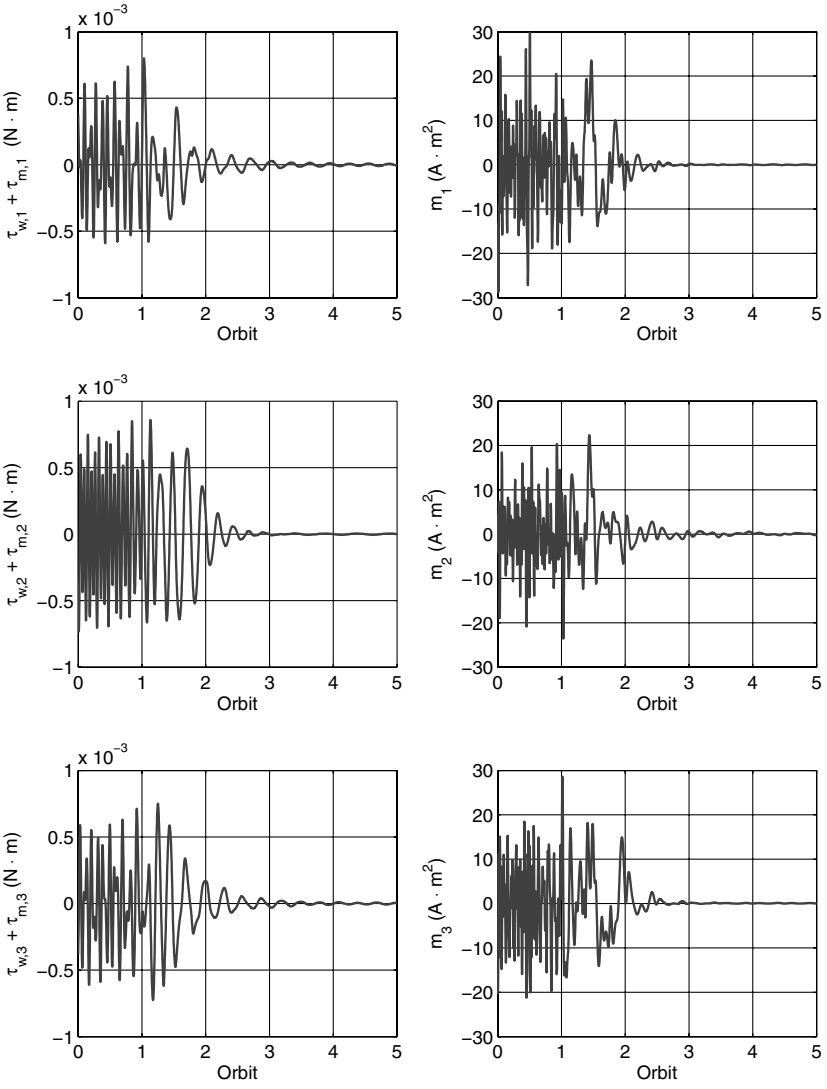

Fig. 3 Combined torque ($\boldsymbol{\tau}_w + \boldsymbol{\tau}_m$) and magnetic dipole moment vs orbit.

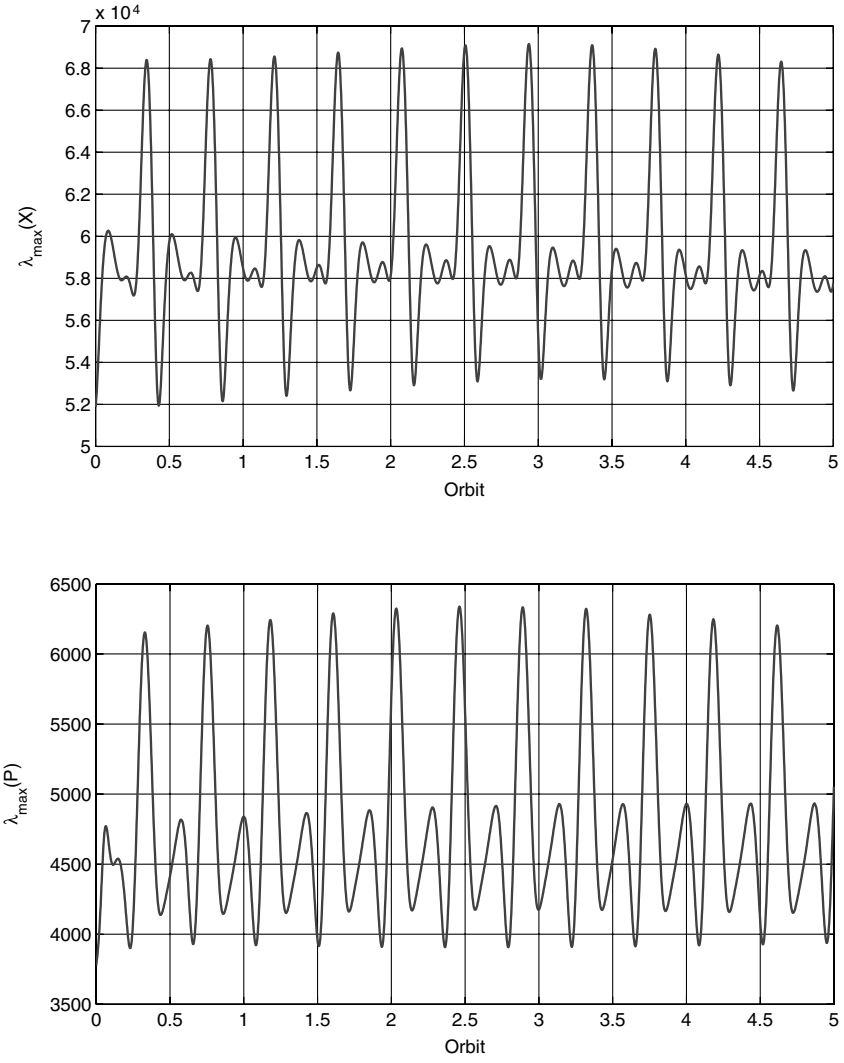

Fig. 4 Maximum eigenvalues of $\mathbf{X}(\cdot)$ and $\mathbf{P}(\cdot)$ vs orbit.

Sec. IV.D is used to design $\mathcal{G}$, robust stability of the spacecraft attitude and angular velocity is assured.

V. Numerical Example

We will consider a spacecraft with moment of inertia matrix $\mathbf{I} = \text{diag}\{27, 17, 25\}$ kg $\cdot$ m^2. It is in a circular Keplerian orbit at an altitude of 450 km and inclination of 87°. The angle of the right ascension of the ascending node, argument of perigee, and time of perigee passage are equal to zero. We will use the magnetic field model described by Wertz [23], Appendix H, and restated in [13].

The spacecraft is equipped with three reaction wheels and three torque rods. The controller is to regulate the quaternions to $\boldsymbol{\epsilon} = \mathbf{0}$, $\eta = 1$, and the angular velocity to $\boldsymbol{\omega} = \mathbf{0}$, while simultaneously rejecting the gravity-gradient disturbance torque of Eq. (2). Control will be computed using the design and synthesis method presented in Sec. IV.D. We will set $k = 7.5 \times 10^{-4}$ N $\cdot$ m and $\delta = 5 \times 10^{-5}$ N $\cdot$ m $\cdot$ s. The LQR weights will be $\mathbf{M} = \text{diag}\{1.5 \times 10^{-3}, 1.5 \times 10^{-3}, 1.5 \times 10^{-3}, 1, 1, 1\}$ and $\mathbf{N} = \text{diag}\{1 \times 10^4, 1 \times 10^4, 1 \times 10^4\}$, while $\mathbf{X}(T) = \mathbf{1}$ where $\mathbf{1}$ is identity. The input strictly passive controller will be weighted by $\mathbf{L} = [\,(1 \times 10^{-8})\mathbf{1} \quad (10)\mathbf{1}\,]$, while we will set $\mathbf{D}_c(t) = [2\delta + (1/80)(-\cos(t/T_0) + 1)]\mathbf{1}$ where T_0 is the orbital period. Letting $\tilde{\mathbf{D}}(t) = [\delta + (1/80)(-\cos(t/T_0) + 1)]\mathbf{1}$, it follows that $\mathbf{W}(t) = \sqrt{2[\delta + (1/80)(-\cos(t/T_0) + 1)]}\mathbf{1}$ by Eq. (7c). Similarly, $\mathbf{P}(T) = \mathbf{1}$, which will be required to solve Eq. (16). The spacecraft initial conditions are $\boldsymbol{\epsilon} = [\,-1/2 \quad 1/2 \quad 1/2\,]^\top$, $\eta = -1/2$, and $\boldsymbol{\omega} = [\,0.02 \quad -0.02 \quad 0.02\,]^\top$ **rad/s**.

Figure 1 shows the angular velocity and quaternion evolution vs time, while Fig. 2 shows the magnetic torques and reaction wheel torques vs time. Figure 3 shows the combined torque $\boldsymbol{\tau}_w + \boldsymbol{\tau}_m$ vs time and the magnetic dipole moments vs time, and Fig. 4 shows the maximum eigenvalues of the matrices $\mathbf{X}(\cdot)$ and $\mathbf{P}(\cdot)$ vs time; notice the nearly periodic nature of both, indicating that the controller is not only time-varying but close to periodic as well. As mentioned in Sec. IV.E, the upper triangular parts of both $\mathbf{X}(\cdot)$ and $\mathbf{P}(\cdot)$ would be approximated using a Fourier series in practice.

The wheel torques do not exceed 1×10^{-3} N $\cdot$ m, the magnetic torques do not exceed 1×10^{-3} N $\cdot$ m, and the magnetic dipole moments do not exceed 30 A $\cdot$ m^2; these values are reasonable. By increasing k, δ, and $\mathbf{M}$ (and decreasing $\mathbf{N}$ or holding it constant), the resultant controller drives the quaternion error and angular velocity error to zero much faster while simultaneously rejecting the gravity-gradient disturbance torque. However, the magnetic dipole moments required are much larger and are practically not possible. The values chosen here are based on various simulations, i.e., tuning. In particular, $\mathbf{M}$ and $\mathbf{N}$ values were first picked given the values presented in [8] and were then tuned.

Recall the general structure of the rate control presented in Eq. (9). Let $\mathbf{u}_{r,w} = -\delta\hat{\mathbf{b}}\hat{\mathbf{b}}^\top\boldsymbol{\omega}$ be the portion of the rate control applied by the reaction wheels and $\mathbf{u}_{r,m} = -\hat{\mathbf{b}}^{\times\top}\mathcal{G}(\hat{\mathbf{b}}^\times\boldsymbol{\omega})$ be the portion applied by the magnetic torque rods. The instantaneous power of the wheels is then $P_w = \boldsymbol{\omega}^\top\mathbf{u}_{r,w}$ while the instantaneous power of the magnetic torque rods is $P_m = \boldsymbol{\omega}^\top\mathbf{u}_{r,m}$. Figure 5 shows the total work done (i.e., the total energy dissipated) by each actuator as a function of time where the total work done is $W_{\text{total}} = \int_0^t P(t')\,\mathrm{d}t'$ and P is P_w or P_m.

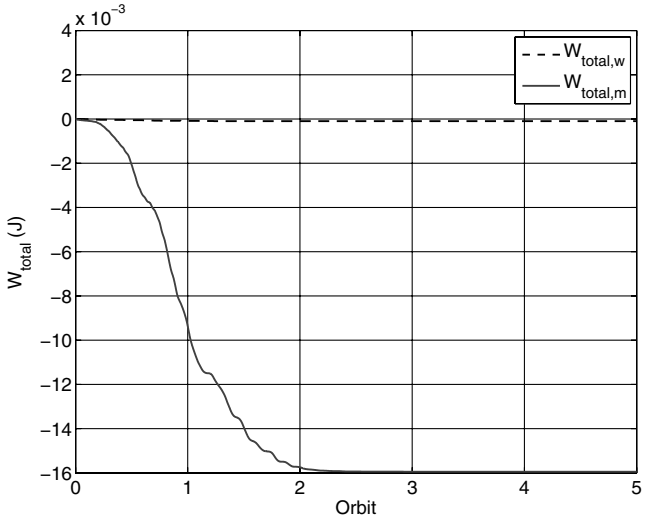

Fig. 5 Total work done by reaction wheels and magnetic torque rods vs orbit.

The total work each actuator does after five orbits is $W_{\text{total,w}} = -9.9324 \times 10^{-5}$ J and $W_{\text{total,m}} = -0.0159$ J. Clearly, the magnetic torque rods dissipate more energy than the reaction wheels do. This in turn means the wheels are not working as hard.

The advantage of our attitude control scheme is that robust stability can be achieved given model uncertainty. This is true given both spacecraft and magnetic field model perturbations. Previous studies conducted employing magnetic actuation alone have only been able to assess the stability of the true system via simulation. For example, [10] perturbs the assumed inertial matrix of the spacecraft by 22% and presents simulations that indicate "some signs of instability." Reference [8] perturbs the spacecraft inertia matrix (by 25 and 30%) and the orbit (by changing the altitude and eccentricity) and is able to show robust stability in simulation.

An example of robust closed-loop stability will be shown next. We will change both the spacecraft inertia properties and orbit. The principal axes of the inertia matrix are reduced by 25%, representing fuel loss, while the altitude, inclination, and eccentricity of the orbit have been changed to 500 km, 67°, and $e = 0.05$, respectively. Figure 6 shows the spacecraft angular velocity and quaternion evolution vs time, given these changes as controlled by the same controller developed for the assumed model and orbit. The system response is only moderately changed, given these significant changes, highlighting the robust nature of the passivity-based control scheme employed.

VI. Conclusions

The attitude control of a spacecraft equipped with both reaction wheels and magnetic torque rods has been considered. It was shown that a spacecraft compensated by quaternion-based proportional control possesses a passive input–output map, enabling the use of an input strictly passive LTV controller to perform rate control. Via the passivity theorem, the spacecraft angular velocity is guaranteed to be stable. Control torques are distributed between reaction wheels and

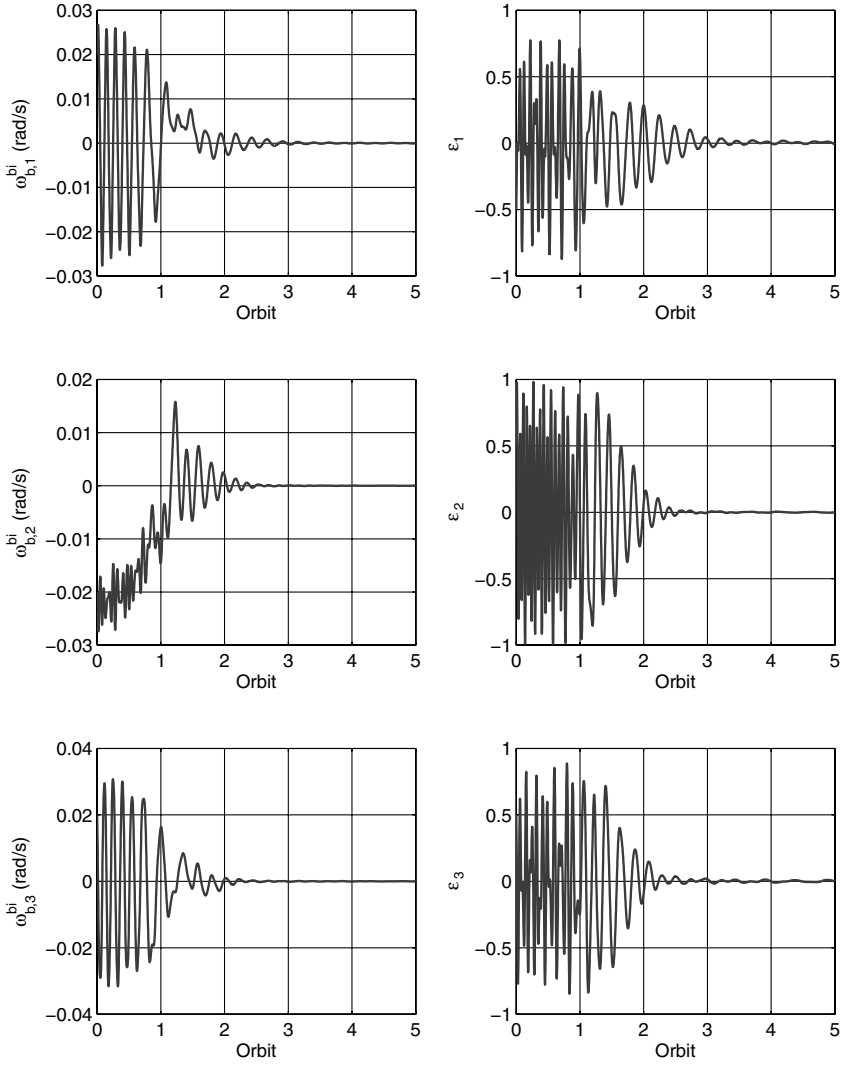

Fig. 6 Angular velocity and quaternion response when spacecraft inertia and orbit have been perturbed.

magnetic torque rods in a natural way guided by the physical constraints imposed by magnetic actuation. To synthesize an input strictly passive controller, the spacecraft plus control distribution architecture is linearized; the linearized state-space model is time-varying. A theorem was presented specifying the form of an LTV input strictly passive system, and it was used, along with the standard LQR formulation, to design an input strictly passive feedback controller based on the linearized system. Using the attitude control scheme presented (i.e., the combination of the proportional and rate control), the vector part of the quaternion and the angular velocity are shown to go to zero at time goes to infinity. Numerical simulation shows this scheme works well, and the controller was found to be nearly periodic.

Although similar ideas to those presented in [13,14] are used, the present work is distinctly different. First, although passivity-based arguments are used in [13], they are used to find the upper bound of a particular gain, not to guarantee closed-loop stability of the nonlinear plant as this paper does. Second, as mentioned previously, in [13] there are no means to guarantee that the reaction wheel torques will not cancel out the magnetic actuation over short periods of time; the present scheme ensures the reaction wheel torques do not overlap with magnetic torques. Third, although the proportional control is distributed between reaction wheels and torque rods using the same decomposition as the one presented [14], the rate control (i.e., the input strictly passive rate control) is distributed differently, which in turn allows for the design of an LTV input strictly passive controller.

Acknowledgments

We would like to thank the associate editor and the anonymous reviewers for their suggestions and comments. We would like to thank Anton de Ruiter, who contributed the results presented in Sec. IV.F.

References

[1] Stickler, A. C. and Alfriend, K. T., "Elementary Magnetic Attitude Control System," *Journal of Spacecraft and Rockets*, Vol. 13, No. 5, 1976, pp. 282–287. doi:10.2514/3.57089

[2] Silani, E., and Lovera, M., "Magnetic Spacecraft Attitude Control: A Survey and Some New Results," *Control Engineering Practice*, Vol. 13, No. 3, 2005, pp. 357–371. doi:10.1016/j.conengprac.2003.12.017

[3] Lovera, M., and Astolfi, A., "Spacecraft Attitude Control Using Magnetic Actuators," *Automatica*, Vol. 40, No. 8, 2004, pp. 1405–1414. doi:10.1016/j.automatica.2004.02.022

[4] Lovera, M., and Astolfi, A., "Global Magnetic Attitude Control of Inertially Pointing Spacecraft," *Journal of Guidance, Control, and Dynamics*, Vol. 28, No. 5, Sept.–Oct. 2005, pp. 1065–1067. doi:10.2514/1.11844

[5] Lovera, M., and Astolfi, A., "Global Magnetic Attitude Control of Spacecraft in the Presence of Gravity Gradient," *IEEE Transactions on Aerospace and Electronic Systems*, Vol. 42, No. 3, July 2006, pp. 796–805. doi:10.1109/TAES.2006.248214

[6] Pittelkau, M., "Optimal Periodic Control for Spacecraft Pointing and Attitude Determination," *Journal of Guidance, Control, and Dynamics*, Vol. 16, No. 6, Nov.–Dec. 1993, pp. 1078–1084. doi:10.2514/3.21130

[7] Wisniewski, R., "Linear Time-Varying Approach to Satellite Attitude Control Using Only Electromagnetic Actuation," *Journal of Guidance, Control, and Dynamics*, Vol. 23, No. 4, July–Aug. 2000, pp. 640–647. doi:10.2514/2.4609

[8] Psiaki, M. L., "Magnetic Torquer Attitude Control via Asymptotic Periodic Linear Quadratic Regulation," *Journal of Guidance, Control, and Dynamics*, Vol. 24, No. 2, March–April 2001, pp. 386–394. doi:10.2514/2.4723

[9] Lovera, M., De Marchi, E., and Bittanti, S., "Periodic Attitude Control Techniques for Small Satellites with Magnetic Actuators," *IEEE Transactions on Control Systems Technology*, Vol. 10, No. 1, Jan. 2002, pp. 90–95. doi:10.1109/87.974341

[10] Wisniewski, R., and Stoustrup, J., "Periodic $\mathcal{H}_2$ Synthesis for Spacecraft Attitude Control with Magnetorquers," *Journal of Guidance, Control, and Dynamics*, Vol. 27, No. 5, Sept.–Oct. 2004, pp. 874–881. doi:10.2514/1.10457

[11] Pulecchi, T., Lovera, M., and Varga, A., "Optimal Discrete-Time Design of Three-Axis Magnetic Attitude Control Laws," *IEEE Transactions on Control Systems Technology*, Vol. 18, No. 3, May 2010, pp. 714–722. doi:10.1109/TCST.2009.2024757

[12] Vigano, L., Bergamasco, M., Lovera, M., and Varga, A., "Optimal Periodic Output Feedback Control: A Continuous-Time Approach and a Case Study," *International Journal of Control*, Vol. 83, No. 5, May 2010, pp. 897–914. doi:10.1080/00207170903487439

[13] Damaren, C. J., "Hybrid Magnetic Attitude Control Gain Selection," *Proceedings of the Institution of Mechanical Engineers, Part G (Journal of Aerospace Engineering)*, Vol. 223, No. 8, 2009, pp. 1041–1047. doi:10.1243/09544100JAERO641

[14] Forbes, J. R., and Damaren, C. J., "Geometric Approach to Spacecraft Attitude Control Using Magnetic and Mechanical Actuation," *Journal of Guidance, Control, and Dynamics*, Vol. 33, No. 2, March–April 2010, pp. 590–595. doi:10.2514/1.46441

[15] Pulecchi, T., and Lovera, M., "Attitude Control of Spacecraft with Partially Magnetic Actuation," *Proceedings of the Seventeenth IFAC Symposium on Automatic Control in Aerospace, Universitas Studii Tolosana, France, June 25 to June 29, 2007*, Vol. 17, No. 1.

[16] Kim, Y., and Deraspe, G., "Resolving RADARSAT-1 Momentum Wheels Failure Problem," *54th International Astronautical Congress of the International Astronautical Federation*, IAC-03-U.4.04, Bremen, Germany, 29 Sept.–3 Oct. 2003.

[17] Roberts, B. A., Kruk, J. W., Ake, T. B., and Englar, T. S., "Three-Axis Attitude Control with Two Reaction Wheels and Magnetic Torquer Bars," AIAA Guidance, Navigation, and Control Conference and Exhibit, AIAA Paper 2004-5245, Providence, RI, 16–19 Aug. 2004.

[18] Desoer, C. A., and Vidyasagar, M., *Feedback Systems: Input–Output Properties*, Academic Press, New York, 1975, Chap. 6, pp. 168–227.

[19] Egeland, O., and Godhavn, J.-M., "Passivity Based Adaptive Attitude Control of a Rigid Spacecraft," *IEEE Transactions on Automatic Control*, Vol. 39, No. 4, 1994, pp. 842–846. doi:10.1109/9.286266

[20] Anderson, B. D. O., and Moore, J. B., "Procedures for Time-Varying Impedance Synthesis," *Proceedings of the 11th Midwest Symposium on Circuit Theory*, May 1968, pp. 17–26.

[21] Anderson, B. D. O., and Moylan, P. J., "Synthesis of Linear Time-Varying Passive Networks," *IEEE Transactions on Circuits and Systems*, Vol. 21, No. 5, Sept. 1974, pp. 678–687. doi:10.1109/TCS.1974.1083926

[22] Hughes, P. C., *Spacecraft Attitude Dynamics*, 2nd ed., Dover, New York, 2004.

[23] Wertz, J. R., *Spacecraft Attitude Determination and Control*, D. Reidel, Dordrecht, The Netherlands, 1978, pp. 779–786.

[24] D'Angelo, H., *Linear Time-Varying Systems: Analysis and Synthesis*, Allyn and Bacon, Boston, 1970, Chap. 4, pp. 93–121.

[25] Zadeh, L. A. and Desoer, C. A., *Linear System Theory: The State Space Approach*, McGraw–Hill, New York, 1963, pp. 512–514.

[26] Lizarralde, F., and Wen, J., "Attitude Control Without Angular Velocity Measurement: A Passivity Approach," *IEEE Transactions on Automatic Control*, Vol. 41, No. 3, March 1996, pp. 468–472. doi:10.1109/9.486654

[27] Kwakernaak, H., and Sivan, R., *Linear Optimal Control Systems*, Wiley-Interscience, Toronto, 1972, pp. 201–203, 216–219.

[28] Bryson, A. E., and Ho, Y.-C., *Applied Optimal Control*, Hemisphere, Toronto, 1975, pp. 148–149.

[29] LaSalle, J. P., "An Invariance Principle in the Theory of Stability," *Control Theory, Twenty-Five Seminal Papers (1932-1981)*, edited by T. Basar, IEEE Publications, Piscataway, NJ, 2001, pp. 309–320.

[30] Khalil, H., *Nonlinear Systems*, 3rd ed., Prentice–Hall, Upper Saddle River, NJ, 2002, pp. 155–156.

[31] Van der Schaft, A., *L_2-Gain and Passivity Techniques in Nonlinear Control*, 2nd ed., Springer, London, 2000, p. 69.

[32] Soltine, J. J. E., and Li, W., *Applied Nonlinear Control*, Prentice–Hall, Upper Saddle River, NJ, 1991, pp. 123–124.